

A REVISED MODEL OF VISUAL RANGE IN FISH

DAG L. AKSNES & ANNE CHRISTINE W. UTNE

SARSIA

AKSNES, DAG L. & ANNE CHRISTINE W. UTNE 1997 08 15. A revised model of visual range in fish. – *Sarsia* 82:137-147. Bergen. ISSN 0036-4827.



Models of visual range and location distances are crucial for quantification of vision based feeding opportunities and predation risk in the pelagic habitat. We compare an earlier published model with measurements of the reactive distance of *Gobiusculus flavescens* relative to two species of copepods. Although this model gave reasonable predictions at low light intensities, the measurements of reactive distance at higher intensities were much lower than those predicted by the model. We modified the model to account for saturation at high light intensities. With this additional feature, the correspondence with the *G. flavescens* observations was significantly improved. Furthermore, the revised model is consistent with earlier published data on fish contrast thresholds obtained over a wide range of target sizes and irradiance levels. Given the values of only two parameters, one sensitivity threshold and one saturation parameter, the model is capable of predicting visual ranges for relatively large intervals of light intensity, prey size and turbidity. Other published visual range models are briefly reviewed and compared with our model.

Dag L. Aksnes & Anne Christine W. Utne, University of Bergen, Department of Fisheries and Marine Biology, Bergen High-Technology Center, N-5020 Bergen, Norway.

KEYWORDS: Predation; feeding; vision; visual range; fish.

INTRODUCTION

In the aquatic environment visual predation is strongly affected by absorption and scattering processes giving rise to poor image transmission and low levels of light intensity. Poor visibility limits the pelagic visual predator in their search for food, but enhances the opportunities for finding refuges for the prey. Because foraging rate and predation risk have great impact on habitat choice, growth and survival (MANGEL & CLARK 1986; 1988; HOUSTON & al. 1993; AKSNES 1996), visual foraging has become an important element of spatial explicit models of fish and plankton (CLARK & LEVY 1988; MASON & PATRICK 1993; ROSLAND & GISKE 1994; TYLER & ROSE 1994; FIKSEN & al. 1995; GISKE & SALVANES 1995; GISKE & al. 1997; ROSLAND in press). The competitive relationship between tactile and visual pelagic predators is severely affected by optical properties of the water column (EIANE & al. in press). The study by KAARTVEDT & al. (1996) demonstrates how horizontal gradients in optical properties can influence distribution and predator-prey interactions of krill and fish.

The vision based encounter process is very sensitive to the visual range of the predator. This range is a complex variable depending on the prey attributes (such as size, contrast and mobility), the visual system of the

predator, as well as on irradiance level, depth and the optical properties of the water (absorption and scattering as related to turbidity and dissolved compounds). A purely empirical approach requires considerable experimentation in order to relate visual range to the relevant factors, and no simple functional relationship seems to fit observations (VINYARD & O'BRIEN 1976). By making assumptions about the functioning of the visual system, mechanistic models of visual range can be formulated (DUNTLEY 1960; 1962; EGGERS 1977; AKSNES & GISKE 1993). Such models encompass two main elements, one stating the criterion necessary for recognition of an object and the other describing the transmission of the image of the object over the sighting distance. One simple recognition criterion says that the apparent contrast of an object has to exceed a contrast threshold in order for the object to be recognised (DUNTLEY 1960; EGGERS 1977). Experimentation on both human and fish vision shows that the use of a constant contrast threshold may be reasonable at high light intensities (CORNSWEET 1970; NICOL 1989), but that the contrast threshold is a variable at lower intensities. Additionally, the contrast threshold also depends on the size of the object. Rather than using the non-dimensional contrast threshold, AKSNES & GISKE (1993) suggested a criterion where contrast, light intensity and

image area all are part of the object recognition criterion. This model, however, was primarily formulated for large depths where the light intensity is low. We will show that the criterion proposed by AKSNES & GISKE (1993) are reasonable at low light intensities, but not at high intensities. By inclusion of a saturation term accounting for characteristics of signal processing and light adaptation processes, however, we will show that a revised version of the model of AKSNES & GISKE (1993) seems consistent with observations of reactive distance in *Gobiusculus flavescens* (UTNE 1997) and contrast thresholds in *Carassius auratus* (HESTER 1968) and *Gadus morhua* (ANTHONY 1981) for a relatively large range of light intensities, object sizes and turbidities.

METHODS

The model

In an earlier paper (AKSNES & GISKE 1993), we assumed that a retinal prey image can only be recognized if the number of photons entering the retina with (F_1) and without (F_2) the image is above a threshold value (ΔS_r).

$$\Delta F = |F_2 - F_1| \geq \Delta S_r \tag{1}$$

It was shown that this is equivalent to the criterion that a prey can only be recognized if the product of retinal prey image contrast (C_r), retinal background irradiance (E_{br}), and area of the retinal prey image (A_{pr}) exceeds the threshold value:

$$|C_r|A_{pr}E_{br} \geq \Delta S_r \tag{2}$$

Table 1. Notation used in the development of the visual range model. Dimensionless quantities are indicated by d.l.

Symbol	Explanation	Unit
A_p	area of the prey	m ²
A_{pr}	area of the prey image at retina	m ²
C_0	inherent contrast of prey	d.l.
C_r	apparent contrast of prey at retina	d.l.
C_t	retinal contrast threshold	d.l.
C_x	apparent contrast of prey at the eye lens	d.l.
c	beam attenuation coefficient	m ⁻¹
ΔF	= $ F_2 - F_1 $	$\mu E \text{ s}^{-1}$
ΔS_e	sensitivity threshold of eye for detection of changes in irradiance	$\mu E \text{ m}^{-2} \text{ s}^{-1}$
ΔS_n	sensitivity threshold for the neural activity	
ΔS_r	sensitivity threshold for detection of changes in radiant flux on retina	$\mu E \text{ s}^{-1}$
E'	= $E_{max} / \Delta S_e$, parameter characterising visual capacity	d.l.
$E_b = E_{bx}$	environmental background irradiance of environmental	$\mu E \text{ m}^{-2} \text{ s}^{-1}$
E_{br}	background irradiance at retina	$\mu E \text{ m}^{-2} \text{ s}^{-1}$
E_{pr}	apparent radiance of prey at retina	$\mu E \text{ m}^{-2} \text{ s}^{-1}$
E_{px}	apparent radiance of prey on eye lens (at distance x)	$\mu E \text{ m}^{-2} \text{ s}^{-1}$
E_{max}	maximal retinal irradiance that can be processed	$\mu E \text{ m}^{-2} \text{ s}^{-1}$
F_1	radiant flux on retina according to background radiance	$\mu E \text{ s}^{-1}$
F_2	radiant flux on retina according to background and prey radiance	$\mu E \text{ s}^{-1}$
f_1	focal length of eye lens	m
K_e	composite saturation parameter reflecting adaptational processes and light /neural activity transformation	$\mu E \text{ m}^{-2} \text{ s}^{-1}$
K_1	maximal neural activity	
K_2	saturation parameter reflecting the transformation of light energy to neural energy	$\mu E \text{ m}^{-2} \text{ s}^{-1}$
k_n	coefficient that converts radiant energy into neural activity	
N	neural activity	
r	visual range	m
x	distance between prey and predator eye lens	m

The subscripts b and p denote the two radiant sources; the background and the prey respectively. The index r refers to the position at the retina (later on, x will refer to the position at the eye lens). By inclusion of eye lens and image transmission characteristics of water, AKSNES & GISKE (1993) arrived at the following non-linear model for the visual range (r):

$$r^2 \exp(cr) = E_b |C_0| A_p \Delta S_e^{-1} \quad (3)$$

where c is the beam attenuation coefficient, C_0 is the inherent contrast of the prey, E_b is the background irradiance (as it appears on the eye lens), A_p is the area of the prey and ΔS_e is a sensitivity threshold for the eye (a composite parameter including several eye-specific characteristics as explained in AKSNES & GISKE 1993). This model was primarily formulated for fish occupying the less illuminated part of the water column. Specifically, this visual range model has been applied in a foraging model of the mesopelagic fish *Maurollicus muelleri* (GISKE & AKSNES 1992; ROSLAND & GISKE 1994), typically experiencing irradiance levels in the range 0.006–0.2 $\mu\text{E m}^{-2}\text{s}^{-1}$ (BALIÑO & AKSNES 1993).

Although not explicitly stated, Eq. (1) assumes that the photons entering the retina give rise to a perceptive neural response that is proportional to the intensity of the incoming light. While this may be an appropriate assumption for the low irradiance levels *M. muelleri* experiences, the neural response becomes weaker as light intensity increases (CORNSWEET 1970). Several processes are likely to contribute to a non-linear transformation of the radiant flux entering the eye. First, theories involving chemical processes, electrical properties of the receptor, and about the effects of various kinds of neural feedback all lead to the prediction that the relationship between the intensity of illumination and the resulting neural activity have the general form (CORNSWEET 1970):

$$N = K_1 \frac{E_{br}}{K_2 + E_{br}} \quad (4)$$

where N is some measure of neural activity, E_{br} is the intensity of the incident light at the visual pigments and K_1 and K_2 are constants. Different kinds of signal processing, such as lateral inhibition, are important in the visual system (CORNSWEET 1970). We do not suggest an explicit representation of such phenomena, but just think of N as a signal that has been modified by different kinds of processing.

In addition to the non-linear transformation of light into neural energy, adaptive processes (such as pigment migration) also contribute to non-linear transformation of the light entering the eye lens. Such adaptational processes reduce the fraction of the ambient light that actually enter the visual pigments. We will assume that the over-all effect of the signal processing and adaptive processes can be described by a relationship similar to that in Eq. (4). Analogous to the criterion (see Eq. 2) used in AKSNES & GISKE (1993), we then formulate:

$$N = k_n |C_r| A_{pr} E_{br} = k_n |C_r| A_{pr} \left[E_{\max} \frac{E_{bx}}{K_e + E_{bx}} \right] \geq \Delta S_n \quad (5a)$$

or

$$|C_r| A_{pr} \left[E_{\max} \frac{E_{bx}}{K_e + E_{bx}} \right] \geq \Delta S_r = \Delta S_n / k_n \quad (5b)$$

Eq. 5b corresponds to Eq. 2, but now a saturation term accounting for non-linear transformation of the light energy is included. k_n is a coefficient converting radiant energy units into neural energy units and E_{\max} represents a maximal retinal irradiance level that can be processed at high ambient irradiance levels (i.e. when $E_b \gg K_e$). Omitting several details (see Appendix) that are described in AKSNES & GISKE (1993), we transform this retinal prey detection criterion to a criterion valid for the irradiance at the eye lens:

$$x^{-2} \exp(-cx) |C_0| A_p E_{\max} \frac{E_b}{K_e + E_b} \geq \Delta S_e \quad (6)$$

where x is the distance between prey and eyelens, c is the beam attenuation coefficient of the water between eye and prey, C_0 is the inherent contrast of the prey, A_p is the size of the prey (measured as an area), and ΔS_e is a species specific sensitivity parameter including lens properties as well as the retinal sensitivity (see AKSNES & GISKE 1993). Now, the visual range (r) is defined by equating left and right hand side of Eq. 6 and setting $x = r$. Rearrangement then gives:

$$r^2 \exp(cr) = |C_0| A_p \frac{E_b}{K_e + E_b} E_{\max} \Delta S_e^{-1} \quad (7)$$

This model corresponds to the visual range model of AKSNES & GISKE (1993). Two new parameters (E_{\max} and K_e), however, have been introduced to account for non-linear transformations of light energy into the neural response. It is convenient to reduce the number of parameters by defining $E' = E_{\max} / \Delta S_e$. Then Eq. 7 becomes:

$$r^2 \exp(cr) = |C_0| A_p E' \frac{E_b}{K_e + E_b} \quad (8)$$

Note that E' is a dimensionless variable characterising the visual capacity of the organism in question.

If the two sensitivity parameters K_e and E' are known, this model predicts the visual range (r) for a given target ($C_0 A_p$) and given environmental conditions (E_b, c). Similarly, if measurements of r are obtained from controlled experiments, estimates of K_e and E' can be obtained.

Comparison of the model with measurements of reactive distance

Reactive distance (R) is frequently used to characterise the visual ability of a predator relative to a prey. UTNE (1997) measured the reactive distance of *Gobiusculus flavescens* relative to the copepods *Acartia longiremis* and *Calanus finmarchicus* at different irradiance and turbidity levels. To compare our model (Eq. 8) with the reactive distance measurements made by UTNE (1997), we assumed that the reactive distance is an indirect measure of the visual range so that $r > R$. The maximal R is a likely estimator for the visual range. However, in order not to depend on a single measurement of r , we defined the 'observed' visual range (r_0) for one experimental set-up as $r_0 = R + 2s$, where R and s are the mean and the standard deviation of the observed reactive distance distribution respectively. Hence, the 'observed' visual range is defined to be a value exceeding about 98 % of the reactive distance observations (see Fig. 1). To compare the model with the observations, the number of parameters in our model had to be reduced. We lumped A_p

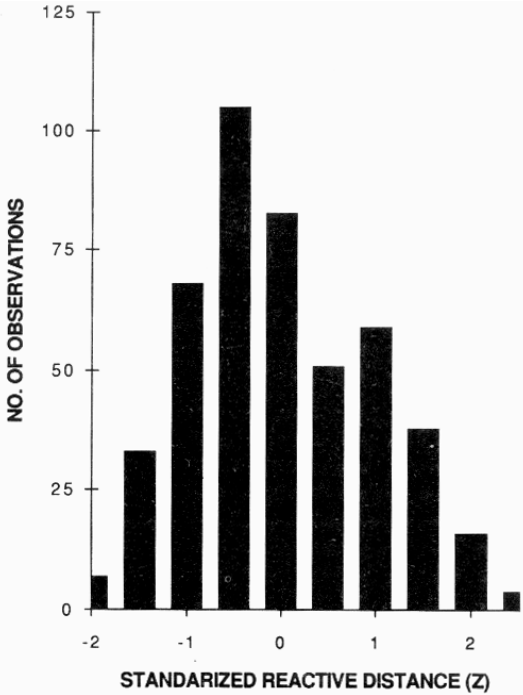


Fig. 1. The standardised distribution of 480 reactive distance measurements in *Gobiusculus flavescens* with *Calanus finmarchicus* as prey item (UTNE 1997) The individual reactive distance measurements were standardised according to $z = (x - R) / s$ where x is the reactive distance, R is the mean reactive distance for one experimental set-up and s is the standard deviation. The visual range (r_0) was defined as $R + 2s$, which corresponds to a standardised reactive distance, $z = 2$.

(prey size), $|C_0|$ (inherent contrast of prey) and E' into a combined parameter, $T_1 = A_p |C_0| E'$. Because we consider prey size and inherent contrast of prey to be constant within each of the two copepod prey experiments, this lumping is appropriate. T_1 can then be interpreted as a prey specific sensitivity parameter. By substitution, Eq. 8 becomes:

$$r_o^2 \exp(cr_o) = T_1 \frac{E_b}{K_e + E_b} \tag{9}$$

Measurements of r_o were carried out at known light intensities (E_b) and at known beam attenuations (c). Hence, estimates of T_1 and K_e could be obtained by fitting Eq. (9) to the observations of r_o . The ability of the model to explain the outcome of the different experiments was visualised by plotting the model predictions together with the measurements (Figs 2; 3).

Calculation of beam attenuation. UTNE (1997) used diatomaceous earth (DE) to generate turbidity in her experiments. The light transmission of the DE-concentrations (JTU) used in the different experiments was measured by a spectrophotometer. We approximated the beam attenuation coefficient from these readings of transmission. The

spectrophotometer had an acceptance half-angle of 1.79° which means that any light that is scattered within 1.79° of the main beam will be detected by the instrument and measured as unattenuated light. Accordingly, the measured transmission (T) is not a function of beam attenuation alone (c , m^{-1}). Forward scattering (b_f , m^{-1}) contributes according to:

$$T = \exp[(b_f - c)l] \tag{10}$$

where l is the thickness of the cuvette (0.1 m). From this expression, we see that increasing forward scattering gives rise to increased measured transmission. ZANEVELD & al. (1979) gave a procedure for correcting observed attenuation for forward scattering. The total scattered light within an angle α (i.e. 1.79°) from the main beam is given by:

$$b_f = 2\pi \int_0^\alpha \beta(\theta) \sin\theta d\theta \tag{11}$$

where $\beta(\theta)$ is the volume scattering function that is approximately constant in the near-forward region. Therefore, by integration:

$$b_f = 2\pi\beta(\theta)(1 - \cos\alpha) \tag{12}$$

Combination of Eq. (10) and (12) gives:

$$c = 2\pi\beta(\theta)(1 - \cos\alpha) - \ln T / l \tag{13}$$

ZANEVELD & al. (1979) measured the near forward scattering function ($\beta(\theta)$) for different turbidity in the range 0-12 JTU. Their values (Table II in ZANEVELD & al. 1979) gave the regression line: $\beta(\theta) = 50.93JTU + 39$ ($r^2 = .98$). By use of this relationship and Eq. (13), we calculated beam attenuation on the basis of the measured transmissions given in UTNE (1997).

Comparison of the model with measurements of contrast threshold

In the contrast threshold measurement experiments made for the goldfish by HESTER (1968) the sighting distance, the beam attenuation and the inherent contrast can be considered constant, while the light intensity and object size were altered systematically. In terms of our model, the retinal contrast threshold (C) can be defined as the minimal contrast necessary for detection. Hence, by use of Eq. (5b), we define the contrast threshold:

$$C_i = \frac{\Delta S_r (K_e + E_b)}{E_{max} A_{pr} D^2 E_b} \tag{14}$$

HESTER (1968) used radiance (F_b , measured in $\mu W \text{ cm}^{-2} \text{ sr}^{-1}$, where sr means steradians) to express light intensity and minutes of arc (min_a) to express the diameter of the object (D). By defining a composite parameter we obtain:

$$C_i = T_2 \frac{(K_e + F_b)}{D^2 F_b} \tag{15}$$

where $T_2 = k\Delta S_r / E_{max}$. Note that the coefficient k appears to account for the different units of our model and the measurements made by HESTER (1968), and for the use of target dia-

meter rather than retinal area in Eq. (15). Nevertheless, our model predicts that T_2 should be invariant to the alterations HESTER (1968) made in radiance level (spanning three orders of magnitude) and object size (spanning two orders of magnitude). Estimates of T_1 and K_e were obtained by fitting Eq. (15) to the C_i observations made by HESTER (1968). The ability of the model to explain the outcome of the different experiments was visualised by plotting the model predictions together with the contrast threshold measurements (Fig. 4).

Correspondingly, the C_i -measurements made for cod by ANTHONY (1981) may also be interpreted in terms of our model. ANTHONY (1981) used only one object size (or rather a combination of different object sizes characterised by a constant total area), and it is therefore appropriate to lump the object area and the sensitivity parameters so that $T_3 = k\Delta S_r / A_{pr} E_{max}$. Eq. (14) then yields (the coefficient k accounts for differences in units):

$$C_i = T_3 \frac{K_e + F_b}{F_b} \quad (16)$$

Our model predicts that T_3 should be invariant to the alterations that ANTHONY (1981) made in radiance level (spanning six orders of magnitude). Estimates of T_3 and K_e were obtained by fitting Eq. (16) to the C_i observations made by ANTHONY (1981). The ability of the model to explain the outcome of the different experiments was visualised by plotting the model predictions together with the contrast threshold measurements (Fig. 5).

RESULTS

Comparison with reactive distance measurements in *Gobiusculus flavescens*

K_e -values of 4 and 5 $\mu\text{E m}^2 \text{s}^{-1}$ were obtained for the *A. longiremis* and *C. finmarchicus* experiments respectively. This indicates that the light saturation of the visual response was independent of the two different objects (see Fig. 2). The T_1 -values were different for the two prey species, $7.5 \cdot 10^{-2}$ (s.d.= $4.0 \cdot 10^{-2}$) and $11.6 \cdot 10^{-2}$ (s.d.= $3.2 \cdot 10^{-2}$) for *C. finmarchicus* and *A. longiremis* respectively. According to the model, T_1 is the product of the inherent contrast, the area of the prey and the sensitivity parameter ($T_1 = A_p |C_0| E$). Hence, it is to be expected that differences in body size and inherent contrasts of the two prey items give different T_1 -values.

Visual range versus light intensity. As can be seen from Fig. 2 the visual range versus irradiance level are well reflected by the model when both *C. finmarchicus* and *A. longiremis* were objects. A rapid initial increase in visual range is followed by a practically constant visual range for further increase in light intensity. As expected, the model without saturation (Eq. 3) corresponds with the measurements of visual range at low light intensities, but becomes

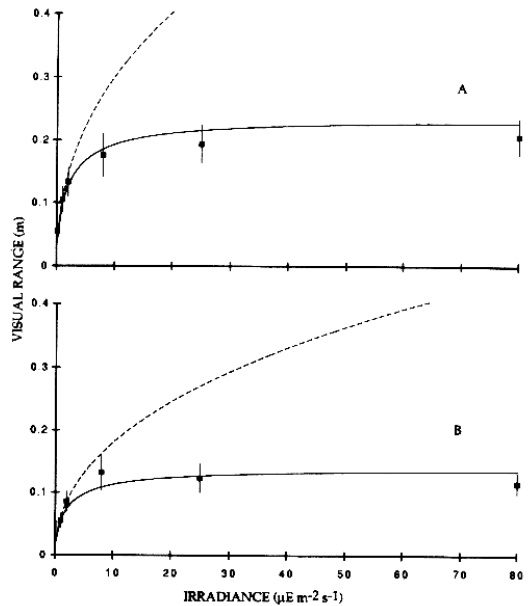


Fig. 2. Observed (± 1 std. dev.) and modelled visual range in *Gobiusculus flavescens* as a function of light intensity and prey (A: *Calanus finmarchicus*, B: *Acartia longiremis*). Solid line represents model with saturation (Eq. 8, $T_1 = 7.5 \cdot 10^{-2}$ and $11.6 \cdot 10^{-2}$ for *C. finmarchicus* and *A. longiremis* respectively, $K_e = 5 \mu\text{E m}^2 \text{s}^{-1}$ for both prey), while broken line represent the model of AKSNES and GISKE (1993) without saturation (Eq. 3).

increasingly biased as the light intensity increases. The retarding increase in visual range with increasing light intensity in this simpler model is caused by the non-linear decrease in retinal image size and apparent contrast with increasing sighting distance. The relationship between visual range and light intensity in the revised model includes a combination of these two effects together with the saturation effect formulated in Eq. 5.

Visual range versus turbidity. At the irradiance level $12 \mu\text{E m}^2 \text{s}^{-1}$, the model reflects the observations of visual range versus turbidity well (Fig. 3a). It should be noted that this comparison was made with the same parameter values (i.e. $T_1 = 7.5 \cdot 10^{-2}$ and $K_e = 5 \mu\text{E m}^2 \text{s}^{-1}$) as in the irradiance experiments (Fig. 2). At the irradiance level $120 \mu\text{E m}^2 \text{s}^{-1}$ use of the same parameter set gave a poorer correspondence. The observed visual range was consistently higher than the modelled at low beam attenuations (Fig. 3b). This discrepancy may indicate a bias in the model, but as discussed by UTNE (1997) it may also be a result of possible contrast enhancement

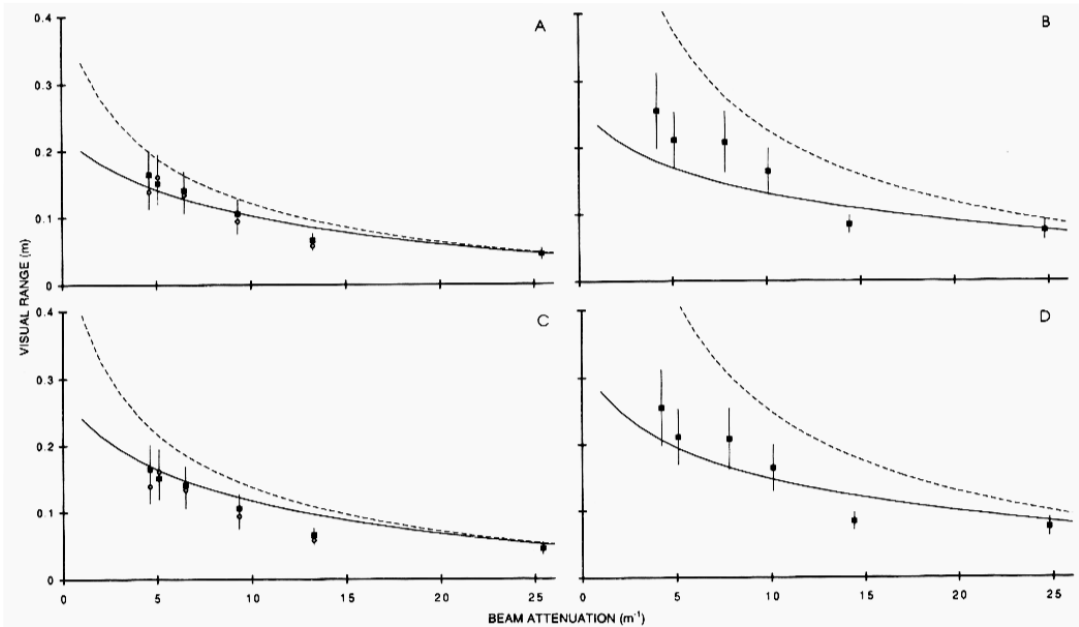


Fig. 3. Observed (± 1 std. dev.) and modelled visual range in *Gobiusculus flavescens* as a function of beam attenuation with *C. finmarchicus* as prey (A,C: at light intensity $12 \mu\text{E m}^{-2} \text{s}^{-1}$ B,D: at light intensity $120 \mu\text{E m}^{-2} \text{s}^{-1}$). Solid line represents the model with saturation (Eq. 8), while broken line represents the model of AKSNES & GISKE (1993) without saturation (Eq. 3). In A and B we have used the same parameter set as in Fig. 2 ($T_1 = 7.5 \cdot 10^{-2}$, $K_c = 5 \mu\text{E m}^{-2} \text{s}^{-1}$), while C and D show the effect of increasing the inherent prey contrast with 50 % (see text for discussion). The different symbols in A and C represents results from two independent experiments.

due to the addition of diatomaceous earth. In Fig. 3c and 3d we have simulated the possible effect of diatomaceous earth mediated increase in inherent contrast (50 % increase) and this resulted in better correspondence with the observations.

Comparison with contrast threshold measurements in *Carassius auratus* (HESTER 1968)

HESTER'S (1968) measurements of contrast threshold were made at four light intensities spanning three orders of magnitude and with five target areas spanning two orders of magnitude (fig. 7 in HESTER 1968). By use of Eq. 15, we estimated $T_2 = 5.8 \cdot 10^2$ and $K_c = 2.0 \mu\text{W cm}^{-2} \text{sr}^{-1}$. The ability of the model to describe the contrast threshold as a function of radiance and target size are demonstrated in Fig. 4. The effect target size makes upon the contrast threshold is well reflected. The relationship between threshold contrast and irradiance level, however, seems somewhat biased since the model consistently underestimates the contrast threshold at the second radiance level. This indicates that a single set of

sensitivity parameters may be unrealistic (see next section).

Comparison with contrast threshold measurements in *Gadus morhua* (ANTHONY 1981)

The contrast thresholds measured by ANTHONY (1981) were obtained over an even larger span in light intensities than those made by HESTER (1968). The background radiance in the experiments ranged from 10^{-7} to $10^{-1} \text{W m}^{-2} \text{sr}^{-1}$. The measurements of C_1 given in ANTHONY (1981, Fig. 5) gave an average $T_2 = 3.19 \cdot 10^{-2}$ and $K_c = 2.9 \cdot 10^{-6} \text{W m}^{-2} \text{sr}^{-1}$. As demonstrated in Fig. 5, use of a single parameter set seems inconsistent with the observations. ANTHONY (1981) noted that the contrast threshold curve showed a discontinuity at a light level of approximately $8 \cdot 10^{-6} \text{W m}^{-2} \text{sr}^{-1}$. This was thought to be linked to the change from photopic (cone based) to scotopic (rod based) vision. Hence, a single set of sensitivity parameters may be unrealistic for light intensities spanning several orders of magnitude. This is demonstrated in Fig. 5 where we included an additional parameter set reflecting improved vision at low light intensities (broken line).

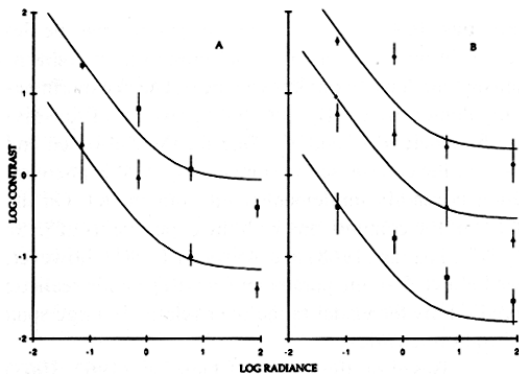


Fig. 4. The modelled (solid line) versus the measured (mean with max. and min. observation) contrast threshold of *Carassius auratus* as (HESTER 1968). (A: size groups 26 (squares) and 92 (triangles) min. of arc, B: size groups 17 (circles), 45 (triangles) and 194 (squares) min. of arc). All modelled lines were generated by $T_2 = 5.8 \cdot 10^2$ and $K_e = 2.0 \mu\text{W cm}^{-2} \text{sr}^{-1}$. Observations are redrawn from Fig. 7 in HESTER (1968). Ranges indicate maximal and minimal observation.

DISCUSSION

As pointed out by WOLKEN (1995) our understanding of how organisms utilise light energy and convert it to chemical, mechanical, and electrical energy is far from complete. The understanding of these processes remains one of the great challenges in biological research. The mechanisms included in models of visual range and reactive distance relative to prey items (DUNTLEY 1963, EGGERS 1977, VINYARD & O'BRIEN 1976, WRIGHT & O'BRIEN 1984, MASON & PATRICK 1993, AKSNES & GISKE 1993) are fragmentary compared to the complexity characterising vision and the optical aquatic environment. Rather than aiming for models covering every aspect of vision and aquatic image transfer, efforts have been directed towards simple representation of some main variables important in the ecological situation, i.e. the prey size, contrast, turbidity and light intensity. The visual pigments and the neural system operate in terms of energy transfer and transformations. Accordingly, it seems appropriate to formulate a perceptual criterion in terms of energy units. Different kinds of light adaptation, lateral retinal inhibition and signal processing diminish the role of light intensity as the signal proceeds through the visual system. Such modifications of the original signal are, in our model, lumped into a single response that is termed light saturation. This is obviously an oversimplification. An central idea in the development of our model, however, was to keep the

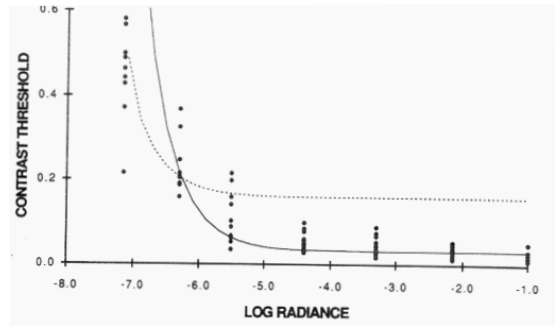


Fig. 5. The modelled versus the measured contrast threshold of *Gadus morhua* (ANTHONY 1981). The solid line was obtained with the parameter values $T_3 = 3.19 \cdot 10^{-2}$ and $K_e = 2.9 \cdot 10^{-6} \text{W m}^{-2} \text{sr}^{-1}$. Broken line indicates the result of increased contrast sensitivity (by lowering T_3 and K_e) at low irradiance levels. Observations are redrawn from Fig. 5 in ANTHONY (1981).

energetic currency of the signal throughout the visual system. This deviates from other approaches where the recognition criterion is based on the dimensionless contrast threshold.

DUNTLEY (1962, 1963) showed that, for horizontal paths of sight, the underwater sighting range of a target is determined by the exponential degradation of the inherent target contrast along the path of sight,

$$C_x = C_0 \exp(-cx) \quad (17)$$

where C_0 and C_x are the inherent and apparent (at distance x) contrast of the target respectively, and c is the beam attenuation constant. With a detailed elaboration of the radiant field distribution, DUNTLEY (1960) provided charts for predicting underwater sighting ranges for objects of different size, transmissions characteristics and depth. It is predicted that not even the most visible object will be seen at distances greater than about 70 m. The recognition criterion was based on data on human visual contrast thresholds provided by TAYLOR (1961).

The focus on the relative difference between the light intensity of the target and the background (as expressed in the contrast definition: $C_x = (E_{px} - E_{bx}) / E_{bx}$), rather than on the absolute intensities of the object and the background, is reasonable because it has been known for a long time that human vision to a large extent is directed

against the perception of the relative difference in intensities. This is expressed in Weber's law stating that the detection threshold difference between the light intensity of a target and the background is directly proportional to the intensity (CORNSWEET 1970). A consequence of this principle is that the absolute difference between the target and background intensities has to be larger at higher than at lower light intensities in order for a target to be recognized (i.e. be distinguished from the background). On the basis of Weber's law, the idea that target recognition is facilitated if the apparent contrast exceeds a specific contrast threshold is appealing. This is in fact how visual range can be calculated for large targets at high (i.e. saturating) light intensities. Under these circumstances the contrast threshold is practically constant. By knowing the contrast threshold (C_t), and ignoring the complicating effect of the angular distribution of light, the visual range is given by $C_t = C_0 \exp(-rc)$ or:

$$r = \ln\left(\frac{C_0}{C_t}\right) / c \tag{18}$$

Basically, Eq. (18) gives the principle of how secchi-disk readings are related to light extinction properties (actually, in this particular application the beam attenuation should be replaced by the sum of the diffuse and the beam attenuation coefficients) although several complications arise by accurate inclusion of the angular distribution of light (PREISENDORFER 1986). According to our model, the contrast threshold is given by:

$$C_t = \frac{K_e + E_b}{A_p E_b E'} = \frac{K_e}{A_p E_b E'} + \frac{E_b}{A_p E_b E'} \tag{19}$$

It can be seen that when the background irradiance (E_b) increases, the contrast threshold approaches a constant value $1/E_p A_p$. Hence, at this point our model is consistent with what is known about contrast thresholds at high light intensities. As shown by Eq. (19), however, our model predicts that the contrast threshold is a variable influenced by the target size as well as the light intensity. The fact that visual range (i.e. reactive distance) of fish increases with increased ambient light intensity is now well documented (O'BRIEN 1987, DOUGLAS & HAWRYSHYN 1990). As pointed out by DOUGLAS & HAWRYSHYN (1990) the light dependent increase in reactive distance is inconsistent with Weber's law. For fish with duplex retinas, plots of threshold contrast (i.e. the Weber fraction) as function of light intensity yield curves that are divisible into two different portions (NICOL 1989). This feature was also discussed by HESTER (1968) and ANTHONY (1981). This is believed to reflect the changeover from predominantly rod to predominantly cone vision being characterised by different sensitivi-

ties. In theory, such changes should also be detected in observations of visual range versus light intensity, but have to our knowledge not been experimentally demonstrated. By introducing two set of sensitivity parameters (E' and K_e), one for the rod-based and one for the cone-based vision (see Fig. 5) this phenomenon is readily implemented into our model. On the basis of the comparisons with the experiments of UTNE (1997), HESTER (1968) and ANTHONY (1981), however, we believe that one parameter set will provide realistic predictions for visual range over relatively large span of light intensities.

Based on the theory of DUNTLEY (1962, 1963) and the experiments of HESTER (1968), EGGERS (1977) formulated a general model for the visual range in fish. He identified three cases for which different criteria for prey recognition should be applied. Case I applies to small prey objects, prey objects of high inherent contrast, and to situations of high levels of ambient illumination or low turbidity:

$$r = \left(\frac{fA_p}{A_{r\min}}\right)^{\frac{1}{2}} \tag{20}$$

where f is the focal length of the eye, A_p is the prey size (area) and $A_{r\min}$ is the minimum retinal image area that can be detected. In Case II that applies to large prey objects or situations of high turbidity or low levels of ambient illumination Eggers applied Eq. (18), but where C_t was a variable as given by the measurements for the Goldfish by HESTER (1968). For situations other than the two above, EGGERS (1977) expressed Case III:

$$C_0 \exp(-cr) = \frac{\delta_1}{(fA_p r^{-2})^{\delta_2}} \tag{21}$$

where δ_1 and δ_2 are constants determined from the experiments of HESTER (1968): $C = \delta_1 / A_{pr}^{\delta_2}$ where A_{pr} is the size of the retinal image.

Our model (Eq. 8) has much in common with the model of EGGERS (1977). Rather than three different criteria, however, we use one criterion for prey recognition. The generality of EGGERS (1977) approach suffers from the fact that the three cases are loosely defined and that the two coefficients δ_1 and δ_2 are not easily interpreted physically or biologically. Under certain circumstances, the use of a single criterion for recognition, as in our model, may be flawed. Case-dependent criteria similar to those of EGGERS (1977) may be more realistic under extreme circumstances. Specifically, consider the situation where the product $|C_t|A_{pr}E_{br}$ is just above the photon flux difference necessary for recognition (i.e. no saturation), and the retinal image size is just above the minimal size necessary for stimulation of

the visual pigments. If we now consider an enlargement of the image area and a simultaneous decrease in light intensity so that the above product remains the same, the model will indicate recognition while the irradiance has fell below the intensity necessary for activating the visual pigment. Hence, in this extreme case it would have been appropriate to carry out individual tests for the retinal resolution and absolute irradiance thresholds.

Much experimental knowledge about how reactive distance in fish is related to environmental variables have been provided by W.J. O'Brien and colleagues. Their research provided the Apparent Size Model (ASM) as an alternative to the widely used Optimal Foraging Theory (OFT) (O'BRIEN & al. 1976, WALTON & al. 1992). VINYARD & O'BRIEN (1976) formulated the following model for the reaction distance (RD, cm) of Bluegill (*Lepomis macrochirus*):

$$RD = PS \left(((\text{Slope} - MS)(1 - (\text{Turbidity}/30))) + MS \right)$$

(22)

$$\text{Slope} = 5.89 - 0.29 \text{ Light} + 19.2 \log_{10} \text{Light}$$

where PS is prey size (mm), Turbidity is given as JTU, Light is the ambient given in lux and MS is a constant. Although this is a model of the reactive distance, rather than of the visual range, all variables accounted for are related to visibility (i.e. it is implicitly assumed that vision is the main variable affecting reactive distance). Similar empirical models have also been specified for the White Crappie (WRIGHT & O'BRIEN 1984) and for the alewife (MASON & PATRICK 1993). Our model behave in many respect similarly to their models: A non-linear response to initial increases in light, linear response to increase in prey size (measured as length rather than area) and a decreasing effect of turbidity as turbidity increases. The effect of visual contrast is not explicitly represented in these models, but enters one or more of the coefficients that have to be experimentally determined.

Visual range, feeding and mortality in pelagic ecology

The present work was primarily motivated from the need for quantitative representation of visual feeding in spatial explicit models of plankton and fish. Traditionally, other aspects of fish feeding, than vision and the optical environment, have received much more attention in the ecological literature. At the encounter level of the predation cycle, swimming speed (GERRITSEN & STRICKLER 1977) and turbulence (ROTHSCHILD & OSBORN 1988, MACKENZIE & al. 1994) are both important elements of the predation process. Analyses also point to

the reactive distance as a most, if not the most, influential parameter of the encounter process. In a sensitivity analysis relating feeding in fish larvae to turbulence, pursuit time and reactive distance, MACKENZIE & al. (1994) demonstrated a huge impact of alterations in the reactive distance on the encounter probability. In this context the findings of WALTON & al. (1992) that the visual volume increased by nearly three orders of magnitude in sunfish between 8 and 50 mm is quite significant for the possibility of accurately determination of potential encounter rates. The environmental impact on visibility makes it very erroneous to assume that the visual range of a predator is fixed over time and depth. Maximal vision based feeding rate (f) for a cruising predator can be expressed (AKSNES & GISKE 1993):

$$f = \frac{h^{-1}N}{\left[h\pi(r \sin \theta)^2 v \right]^{-1} + N} \quad (23)$$

where h is the time needed for handling of a prey item, N is the prey abundance, v is the cruising speed of the predator (turbulence and prey motility, however, will also enter this parameter), θ is the reaction field half angle and r is the visual range given by Eq. 8 (or Eq. 3 if the model without saturation is considered). Although other aspects of the predation cycle such as pursuit, attack, retention and stochasticity should not be underrated, we will restrict ourselves to a discussion of factors affecting the maximal vision based feeding rate.

The light level at depth z can be expressed:

$$E_z = E_0 \exp(-Kz) \quad (24)$$

where E_0 is the irradiance just below the surface, and K is the diffuse attenuation coefficient. By equating the background irradiance (E_b) in Eq. 8 with E_z , visual range and maximal feeding rate can be represented as a function of depth (and surface irradiance). Such representation is primarily recommended for large depths where the radiance field is fairly uniform. AKSNES & GISKE (1993) concluded that the vision based feeding rate of *Maurollicus muelleri* at 125 m depth could span several order of magnitude as a result of characteristic variations in the light regime (daytime E_0 and K), while characteristic variability in prey abundance had much lesser influence on the feeding rate.

The strong impact light conditions have on feeding, growth, habitat choice, and fitness of fish and zooplankton is demonstrated in the optimisation models of CLARK & LEVY (1988), ROSLAND & GISKE (1994, 1997) and FIKSEN & GISKE (1995). The realism of such models, and spatial explicit fish population model in general (BRANDT & KIRSCH 1993, TYLER & ROSE 1994,

FIKSEN & al. 1995), however, strongly depend on the parameterisation of the visual ability. On the basis of fitness maximisation one should expect that spatial gradients in predation risk often make stronger impact on habitat choice and animal distribution than gradients in feeding opportunities (AKSNES & GISKE 1990, GISKE & al. 1994). Hence, in an ecological context, modelling of visual range serve two purposes: Representation of vision based feeding and vision based predation risk, both central elements of unified foraging theory (MANGEL & CLARK 1986) as well as of the aquatic environment itself.

ACKNOWLEDGMENTS

We thank Ø. Fiksen, P. Caparroy, J. Giske and an anonymous reviewer for valuable comments on the manuscript. This work has been supported by grant from the Research Council of Norway.

APPENDIX

DERIVATION OF EQ. (6)

We assume that the retinal contrast (C_r) is proportional (or equal) to the apparent contrast (C_x) at the eye lens:

$$C_r = kC_x \quad (A1)$$

The apparent contrast at the eye lens is related to the inherent contrast (DUNTLEY, 1962):

$$C_x = C_0 \exp(-cx) \quad (A2)$$

where c is the beam attenuation coefficient, and C_0 is the inherent contrast of the prey. The image area (A_{pr}) of the prey on retina is related to the real area (A_p) of the prey by:

$$A_{pr} = \frac{A_p f^2}{x^2} \quad (A3)$$

where x is the distance between eye lens and prey, and f is focal length of the lens. In order to omit detailed parameterization of eye optics, we define:

$$\Delta S_e = \frac{\Delta S_r}{kf^2} \quad (A4)$$

Thus, three parameters concerning the eye are lumped into a single eye-specific sensitivity parameter (ΔS_e) which has the unit of irradiance (at the eye). By use of Eqs. (A1-A4), Eq. 5b becomes:

$$x^{-2} \exp(-cx) C_0 \left| A_p E_{\max} \frac{E_b}{K_e + E_b} \right| \geq \Delta S_e \quad (A5)$$

which is identical to Eq. 6.

REFERENCES

- Aksnes, D.L. 1996. Natural mortality, fecundity and development time in marine planktonic copepods - implications of behaviour. – *Marine Ecology Progress Series* 131:315-316
- Aksnes, D.L. & J. Giske 1990. Habitat profitability in pelagic environments. – *Marine Ecology Progress Series* 64:209-215.
- 1993. A theoretical model of visual aquatic predation. – *Ecological Modelling* 67:233-250.
- Anthony, P.D. 1981. Visual contrast thresholds in the cod *Gadus morhua* L. – *Journal of Fish Biology* 19:87-103.
- Baliño, B.M. & D.L. Aksnes 1993. Winter distribution and migration of the sound scattering layers, zooplankton and micronekton in Masfjorden, western Norway. – *Marine Ecology Progress Series* 102:35-50.
- Brandt, S.B. & J. Kirsch 1993. Spatially explicit models of Striped Bass growth potential in Chesapeake Bay. – *Transactions of the American Fisheries Society* 122:845-869.
- Clark, C.W. & D.A. Levy 1988. Diel vertical migration by juvenile sockeye salmon and the antipredation window. – *American Naturalist* 131:271-290.
- Cornsweet, T.N. 1970. *Visual perception*. – Academic Press, Inc. London. 475 pp.
- Douglas, R.H. & C.W. Hawryshyn 1990. Behavioural studies of fish vision: an analysis of visual capabilities. – Pp. 373-418 in: Douglas, R.H. & M. Djamgoz (eds) *The visual system of fish*. Chapman & Hall, Cambridge.
- Duntley, S.Q. 1960. Improved nomographs for calculating visibility by swimmers (natural light). – Bureau of Ships Contract No. bs-72039, Rep. 5-3 Feb.
- 1962. Underwater visibility. – Pp. 452-455 in: Hill, M.N. (ed) *The Sea*. Vol. 1. J. Wiley & Sons, London.
- 1963. Light in the sea. – *Journal of the Optical Society of America* 53:214-233.
- Eggers, D.M. 1977. The nature of prey selection by planktivorous fish. – *Ecology* 58:46-59.
- Eiane, K., D.L. Aksnes, & J. Giske 1997. The significance of optical properties in competition among visual and tactile planktivores: a theoretical study. – *Ecological Modelling* 98:123-136.
- Fiksen, Ø. & J. Giske 1995. Vertical distribution and population dynamics of copepods by dynamic optimization. – *ICES Journal of Marine Science* 52:483-503.
- Fiksen, Ø., J. Giske, & D. Slagstad 1995. A spatially explicit fitness-based model of capelin migrations in the Barents Sea. – *Fisheries Oceanography* 4:193-208.
- Gerritsen J. & J.R. Strickler 1977. Encounter probabilities and community structure in zooplankton: a mathematical model. – *Journal of Fisheries Research Board of Canada* 34:73-82.
- Giske, J. & D.L. Aksnes 1992. Ontogeny, season and trade-offs: vertical distribution of the mesopelagic fish *Maurollicus muelleri*. – *Sarsia* 77:253-262.
- Giske, J., D. L. Aksnes, & Ø. Fiksen 1994. Visual predators, environmental variables and zooplankton mortality risk. – *Vie & Milieu* 44:1-9

- Giske, J., R. Rosland, J. Berntsen, & Ø. Fiksen 1997. Ideal free distribution of copepods under predation risk. – *Ecological Modelling* 95:45-59.
- Giske, J. & A.G.V. Salvanes 1995. Why pelagic planktivores should be unselective feeders. – *Journal of theoretical Biology* 173:41-50.
- Gregory, R.S. & T.G. Northcote 1993. Surface, planktonic, and benthic foraging by juvenile Chinook salmon (*Oncorhynchus tshawytscha*) in turbid laboratory conditions. – *Canadian Journal of Fisheries and Aquatic Sciences* 50:233-240.
- Hester, F.J. 1968. Visual contrast thresholds of the Goldfish (*Carassius auratus*). – *Vision Research* 8:1315-1335.
- Houston, A.I., J.M. McNamara, & J.M.C. Hutchinson 1993. General results concerning the trade-off between gaining energy and avoiding predation. – *Philosophical Transactions of the Royal Society of London Series B* 341:375-397.
- Kaartvedt, S., W. Melle, T. Knutsen & H.R. Skjoldal 1996. Vertical distribution of fish and krill beneath water of varying optical properties. – *Marine Ecology Progress Series* 136:51-58.
- MacKenzie, B.R., T.J. Miller, S. Cyr & W.C. Leggett 1994. Evidence for a dome-shaped relationship between turbulence and larval fish ingestion rates. – *Limnology & Oceanography* 39:1790-1799.
- Mangel, M. & C.W. Clark 1986. Towards a unified foraging theory. – *Ecology* 67: 1127-1138.
- 1988. *Dynamic modelling in behavioural ecology*. – Princeton University Press, Princeton, NJ. 308 pp.
- Mason, D.M. & E. V. Patrick 1993. A model for the space-time dependence of feeding for pelagic fish populations. – *Transactions of the American Fisheries Society* 122:884-901.
- Miner, G.J. & R.A. Stein 1993. Interactive influence of turbidity and light on larval Bluegill (*Lepomis macrochirus*) foraging. – *Canadian Journal of Fisheries and Aquatic Sciences* 50:781-788.
- Nicol, J.A.C. 1989. *The eyes of fishes*. – Clarendon Press, Oxford. 308 pp.
- O'Brien, W.J., N.A. Slade, & G.L. Vinyard 1976. Apparent size as determinant of prey selection by bluegill sunfish (*Lepomis macrochirus*). – *Ecology* 57:1304-1310.
- O'Brien, W.J. 1987. Planktivory by freshwater fish: Thrust and parry in pelagia. – Pp. 3-16 in: Kerfoot, W.C. & A. Sih (eds). *Predation: Direct and indirect impacts on aquatic communities*. University Press of New England, Hanover.
- Preisendorfer, R.W. 1986. Secchi disc science: Visual optics of natural waters. – *Limnology & Oceanography* 31:909-226.
- Rosland, R. & J. Giske 1994. A dynamic optimization model of the diel vertical distribution of a pelagic planktivorous fish. – *Progress in Oceanography* 34:1-43.
- 1997. A dynamic model for the life history of *Maurolicus muelleri*, a pelagic planktivore fish. – *Fisheries Oceanography* 6:19-34.
- Rosland, R. 1997. Optimal responses to environmental and physiological constraints: evaluation of a model for a planktivore. – *Sarsia* 82:113-128.
- Rothschild, B.J. & Osborn 1988. Small-scale turbulence and plankton contact rates. – *Journal of Plankton Research* 10:465-474.
- Taylor, J.H. 1961. Contrast-thresholds as a function of retinal position and target size for the light-adapted eye. – *University of California, Vision Laboratory SIO ref. SIO 61-10*.
- Tyler, J.A. & K.A. Rose 1994. Individual variability and spatial heterogeneity in fish population models. – *Reviews in Fish Biology and Fisheries* 4:91-123.
- Utne, A.C.W. 1997. The effect of turbidity and illumination on the reaction distance and search time of a marine planktivore (*Gobiusculus flavescens*). – *Journal of Fish Biology* 50:926-938.
- Vinyard, G.L. & W.J. O'Brien 1976. Effects of light and turbidity on the reactive distance of Bluegill (*Lepomis macrochirus*) – *Journal of Fisheries Research Board of Canada* 33:2845-2849.
- Walton, W.E., N.G. Hairston, & J.K. Wetterer 1992. Growth-related constraints on the diet selection by sunfish. – *Ecology* 73:429-437.
- Wolken, J.J. 1995. *Light detectors, photoreceptors, and imaging systems in nature*. – Oxford University Press, Oxford. 259 pp.
- Wright, D.I. & W.J. O'Brien 1984. The development and field test of a tactical model of the planktivorous feeding of white crappie (*Pomoxis annularis*). – *Ecological Monographs* 54:65-98.
- Zaneveld, J.R.V., R.W. Spinrad, & R. Bartz 1979. Optical properties of turbidity standards. – *Ocean Optics* 6:159-168.

Accepted 3 June 1997

